Supplementary Information for:

An immunosuppressed microenvironment distinguishes lateral ventricle-contacting glioblastomas
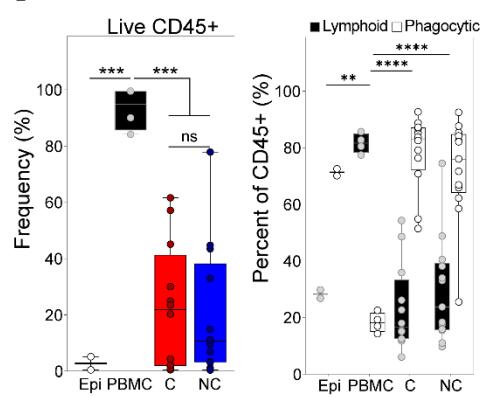
Todd Bartkowiak[1,2,3], Sierra M. Lima[1,2], Madeline J. Hayes[1,2], Akshitkumar M. Mistry[3,4], Asa A. Brockman[1], Justine Sinnaeve[1,3], Nalin Leelatian[1,2,3], Caroline E. Roe[1,2,3], Bret C. Mobley[2,3], Silky Chotai[4], Kyle D. Weaver[3,4], Reid C. Thompson[3,4], Lola B. Chambless[3,4], Rebecca A. Ihrie[1,3,5]*, Jonathan M. Irish[1,2,3]*
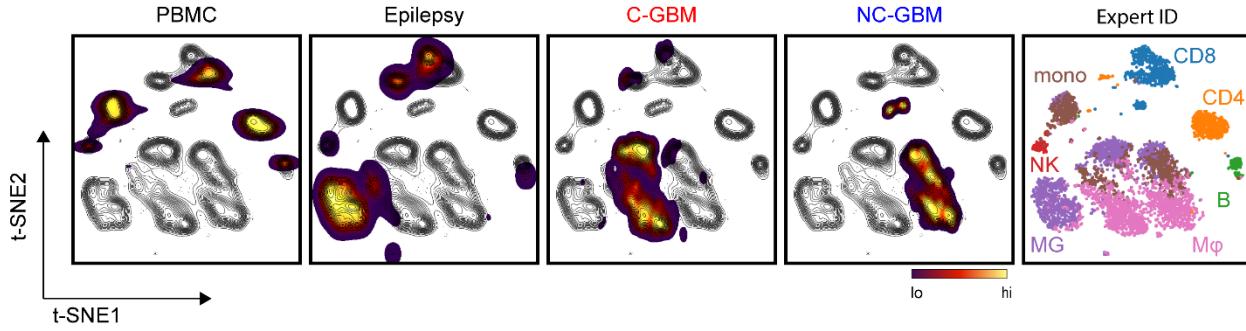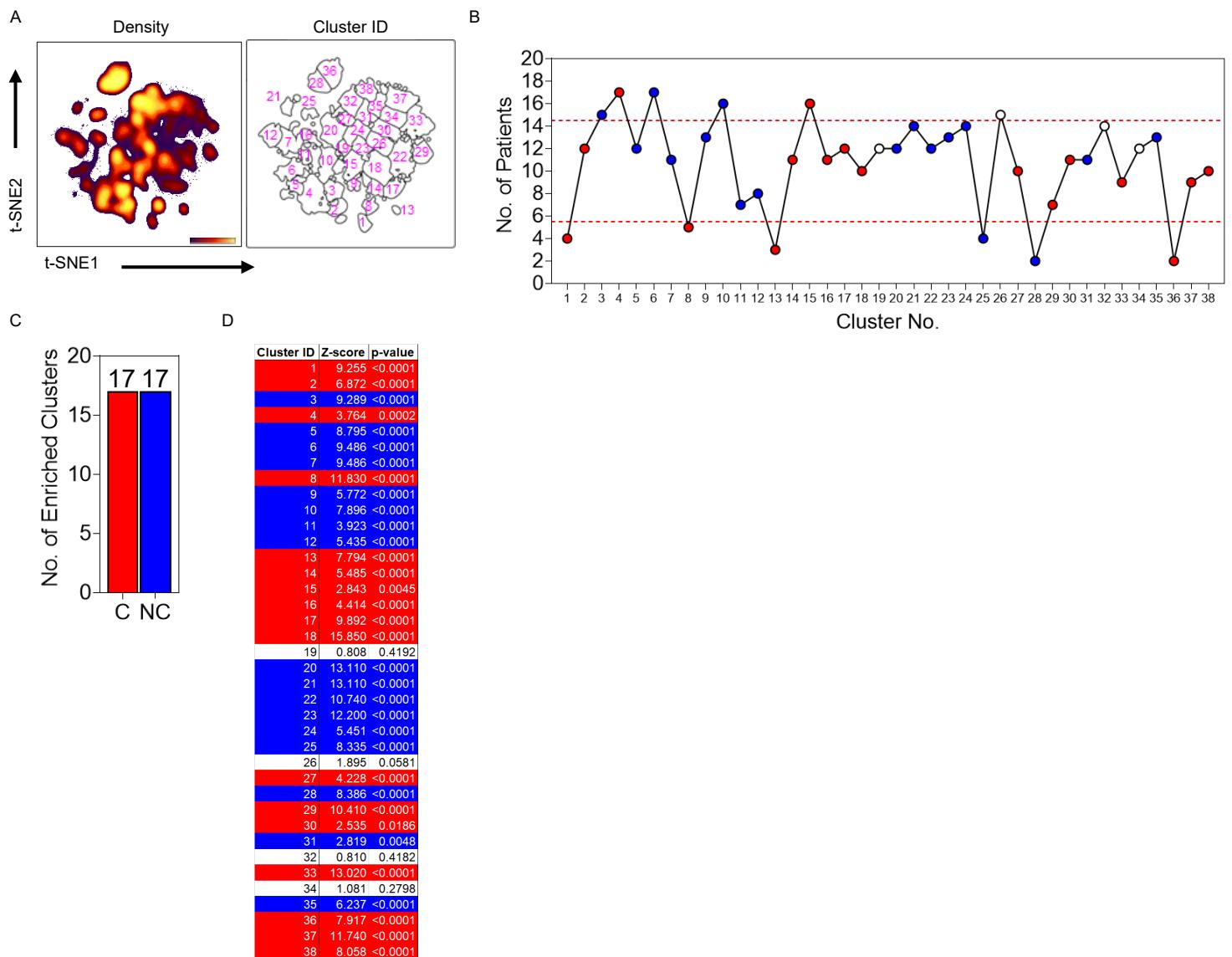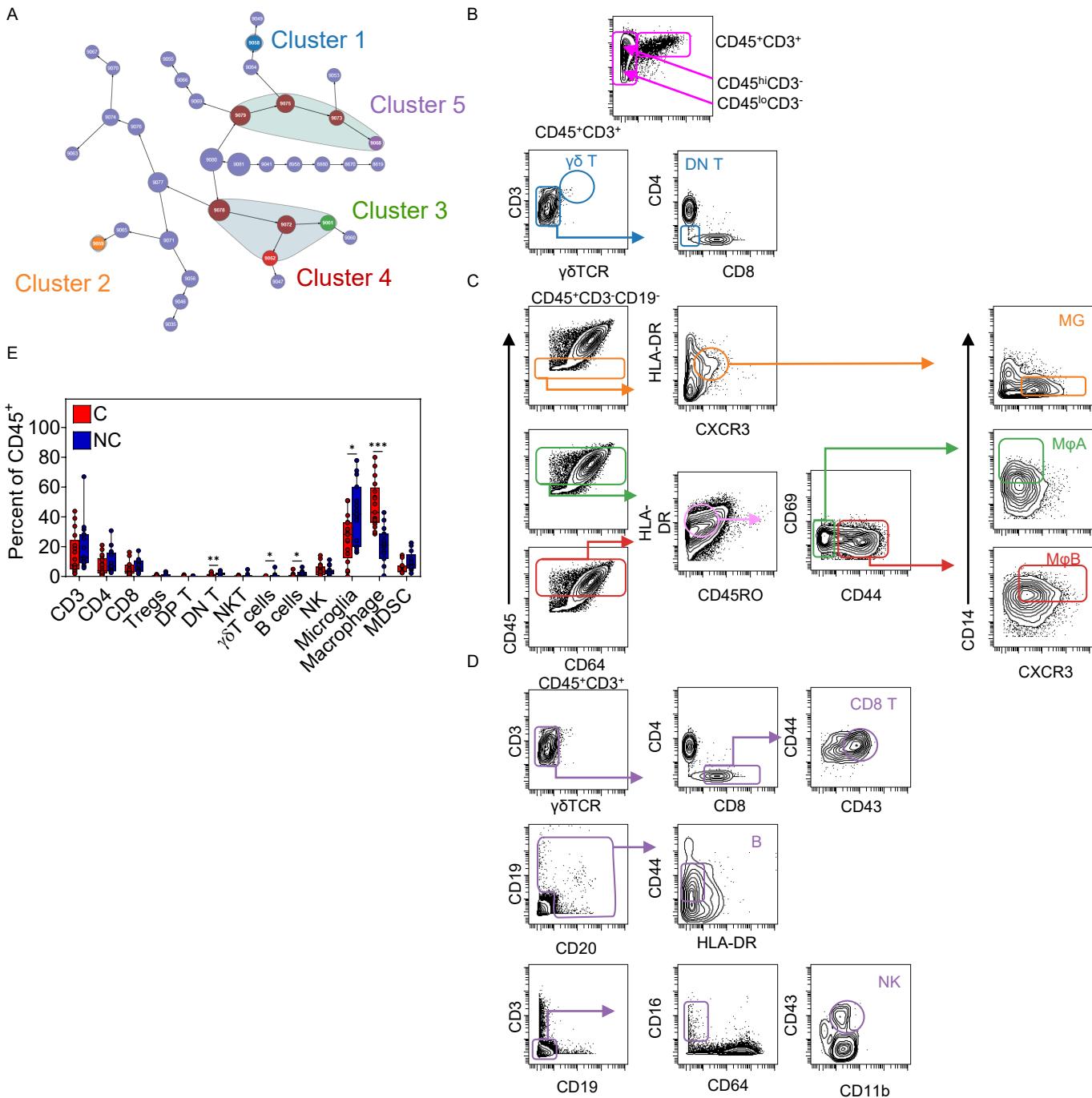
Supplementary Figure 1: Quantification of immune infiltration in GBM. A) Box and whisker plots demonstrating the frequency of expert-gated immune populations in epileptic brain (white, n=2), healthy donor PBMC (dark grey, n=4), or glioblastoma tumors (light grey, n=25). B) Box and whisker plots demonstrating the total leukocyte infiltration (left) and lymphoid and phagocytic fractions (right) in epileptic brain (Epi), healthy donor blood (PBMC), C-GBM (C) or NC-GBM (NC). C) Representative t-SNE plots of all CD45+ leukocytes identified in the blood, non-tumor bearing brain, or GBM tumors (heat) overlaid onto all pooled CD45+ events. Multi-color overlay represents expert gated populations overlaid onto the t-SNE axes. Bars in A and B indicate median ± IQR. Statistical significance in A and B were calculated using a 2-way ANOVA with Sidak's multiple comparison's test from n=12 C-GBM and n= 13 NC-GBM. * = p<0.05, ** = p<0.01, *** = p<0.001, **** = p <0.0001.

Supplementary Figure 2
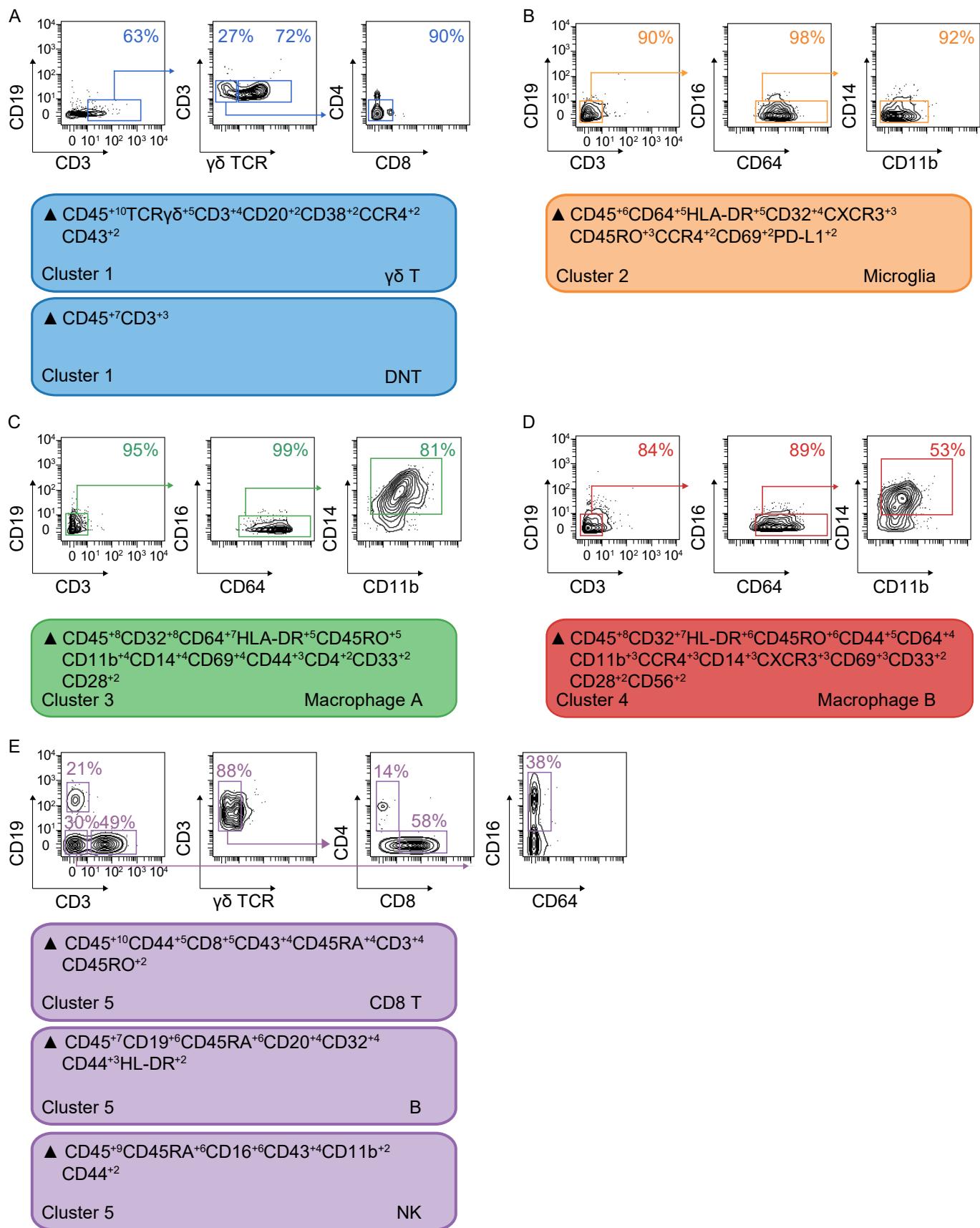
Supplementary Figure 2: Computational determination of enriched immune populations in C-GBM and NC-GBM tumors. A) t-SNE plots indicating the density (left) and FlowSOM cluster enumeration of CD45+ cells pooled from 19/32 GBM patients. B) Graphical representation of the number of patients represented within each FlowSOM cluster. Dotted red lines indicate the 25th and 75th percentile respectively. Red dots indicate a statistical enrichment of C-GBM patients, blue dots indicate enrichment of NC-GBM patients in each cluster, and white dots indicate non-enriched clusters. C) Bar graph representing the number of total clusters statistically enriched in patients with C-GBM or NC-GBM tumors. D) Chart indicating the Z-scores and p-values from Chi-squared analysis to determine statistical enrichment of cells from C-GBM (red) or NC-GBM patients for each cluster.

Supplementary Figure 3

Supplementary Figure 3: Identified Citrus clusters correspond to lymphoid and phagocytic immune subsets. A) Citrus clustergram of statistically enriched immune cell populations. Circled maroon nodes indicate clusters of differential abundance. Color coded nodes indicate terminal nodes used for further analysis. B-D) Representative expert-guided biaxial gates identifying immune cells subsets identified by Citrus in 6/32 patients not included in Citrus analysis. E) Box and whisker plots showing the frequency of each indicated expert-gated immune population as a percent of total CD45+ tumor infiltrating leukocytes from n=13 NC-GBM and n=12 C-GBM. Gating strategies in B-D were defined by MEM labels and the most distinguishing features for each Citrus subset. Quantification in E represents manually gated populations from 25/32 patients in the cohort. Statistical significance in E was determined using an unpaired t-test with Welch's correction for multiple comparisons and a FDR<0.01. * = p<0.05, ** = p<0.01, *** = p<0.001, **** = p <0.0001.

A

CD19 / CD3 — 63%
CD3 / γδ TCR — 27% 72%
CD4 / CD8 — 90%

▲ CD45^{+10}TCRγδ^{+5}CD3^{+4}CD20^{+2}CD38^{+2}CCR4^{+2}
CD43^{+2}

Cluster 1 — γδ T

▲ CD45^{+7}CD3^{+3}

Cluster 1 — DNT

B

CD19 / CD3 — 90%
CD16 / CD64 — 98%
CD14 / CD11b — 92%

▲ CD45^{+6}CD64^{+5}HLA-DR^{+5}CD32^{+4}CXCR3^{+3}
CD45RO^{+3}CCR4^{+2}CD69^{+2}PD-L1^{+2}

Cluster 2 — Microglia

C

CD19 / CD3 — 95%
CD16 / CD64 — 99%
CD14 / CD11b — 81%

▲ CD45^{+8}CD32^{+8}CD64^{+7}HLA-DR^{+5}CD45RO^{+5}
CD11b^{+4}CD14^{+4}CD69^{+4}CD44^{+3}CD4^{+2}CD33^{+2}
CD28^{+2}
Cluster 3 — Macrophage A

D

CD19 / CD3 — 84%
CD16 / CD64 — 89%
CD14 / CD11b — 53%

▲ CD45^{+8}CD32^{+7}HL-DR^{+6}CD45RO^{+6}CD44^{+5}CD64^{+4}
CD11b^{+3}CCR4^{+3}CD14^{+3}CXCR3^{+3}CD69^{+3}CD33^{+2}
CD28^{+2}CD56^{+2}
Cluster 4 — Macrophage B

E

CD19 / CD3 — 21% 30% 49%
CD3 / γδ TCR — 88%
CD4 / CD8 — 14% 58%
CD16 / CD64 — 38%

▲ CD45^{+10}CD44^{+5}CD8^{+5}CD43^{+4}CD45RA^{+4}CD3^{+4}
CD45RO^{+2}

Cluster 5 — CD8 T

▲ CD45^{+7}CD19^{+6}CD45RA^{+6}CD20^{+4}CD32^{+4}
CD44^{+3}HL-DR^{+2}

Cluster 5 — B

▲ CD45^{+9}CD45RA^{+6}CD16^{+6}CD43^{+4}CD11b^{+2}
CD44^{+2}

Cluster 5 — NK

Supplementary Figure 4. Expert-guided confirmation of Citrus-identified immune populations. Representative biaxial gating of pooled Citrus clusters and Marker Enrichment Modeling (MEM) population identification classified each cluster as (A) γδ and CD4$^-$CD8$^-$ DNT cells, (B) microglia, (C) and (D) macrophages and (E) lymphocyte populations of CD8 T cells, B cells and NK cells.

A

B

Supplementary Figure 5: Quantification of tumor-infiltrating immune cells with multiplex IHC. A) Representative immunohistochemistry micrographs indicating immune infiltration into the tumor parenchyma. B) Quantification of indicated immune cell frequencies identified by CyTOF mass cytometry and matched multiplexed immunohistochemistry (n=6). Scale bars indicate 100 µm. Statistical significance in B was calculated using a paired Student's T test.
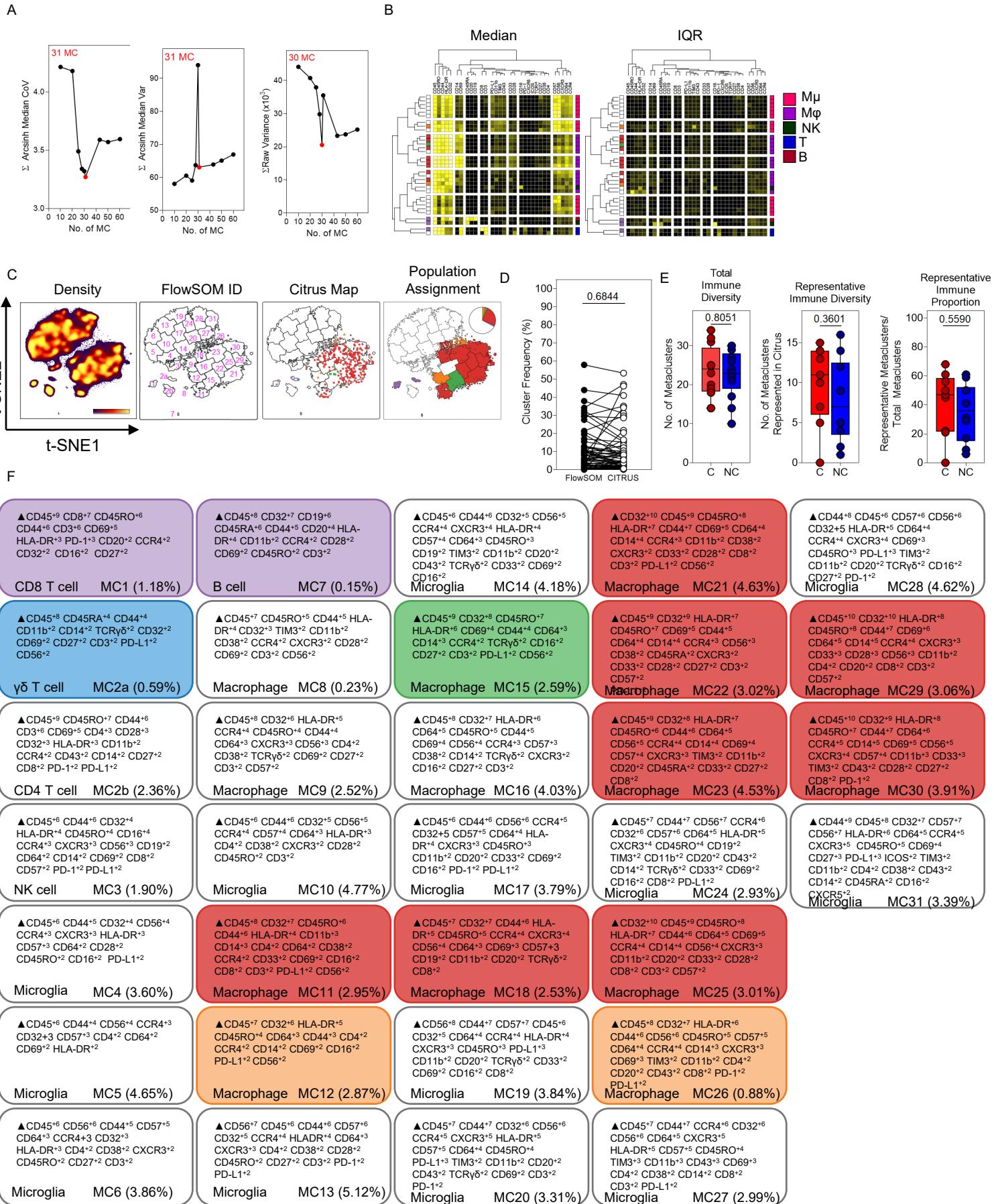
Supplementary Figure 6

A

B   Median   IQR

C   Density   FlowSOM ID   Citrus Map   Population Assignment

D

E   Total Immune Diversity   Representative Immune Diversity   Representative Immune Proportion/Total Metaclusters

F

▲CD45+9 CD8+7 CD45RO+6 CD44+6 CD3+6 CD69+5 HLA-DR+3 PD-1+3 CD20+2 CCR4+2 CD32+2 CD16+2 CD27+2
CD8 T cell   MC1 (1.18%)

▲CD45+8 CD32+7 CD19+6 CD45RA+6 CD44+5 CD20+4 HLA-DR+4 CD11b+2 CCR4+2 CD28+2 CD69+2 CD45RO+2 CD3+2
B cell   MC7 (0.15%)

▲CD45+6 CD44+6 CD32+5 CD56+5 CCR4+4 CXCR3+4 HLA-DR+4 CD57+4 CD64+3 CD45RO+3 CD19+2 TIM3+2 CD11b+2 CD20+2 CD43+2 TCRγδ+2 CD33+2 CD69+2 CD16+2
Microglia   MC14 (4.18%)

▲CD32+10 CD45+9 CD45RO+8 HLA-DR+7 CD44+7 CD69+5 CD64+4 CD14+4 CCR4+3 CD11b+2 CD38+2 CXCR3+2 CD33+2 CD28+2 CD8+2 CD3+2 PD-L1+2 CD56+2
Macrophage   MC21 (4.63%)

▲CD44+8 CD45+6 CD57+6 CD56+6 CD32+5 HLA-DR+5 CD64+4 CCR4+4 CXCR3+4 CD69+3 CD45RO+3 PD-L1+3 TIM3+2 CD11b+2 CD20+2 TCRγδ+2 CD16+2 CD27+2 PD-1+2
Microglia   MC28 (4.62%)

▲CD45+8 CD45RA+4 CD44+4 CD11b+2 CD14+2 TCRγδ+2 CD32+2 CD69+2 CD27+2 CD3+2 PD-L1+2 CD56+2
γδ T cell   MC2a (0.59%)

▲CD45+7 CD45RO+5 CD44+5 HLA-DR+4 CD32+3 TIM3+2 CD11b+2 CD38+2 CCR4+2 CXCR3+2 CD28+2 CD69+2 CD3+2 CD56+2
Macrophage   MC8 (0.23%)

▲CD45+9 CD32+8 CD45RO+7 HLA-DR+6 CD69+4 CD44+4 CD64+3 CD14+3 CCR4+2 TCRγδ+2 CD16+2 CD27+2 CD3+2 PD-L1+2 CD56+2
Macrophage   MC15 (2.59%)

▲CD45+9 CD32+9 HLA-DR+7 CD45RO+7 CD69+5 CD44+5 CD64+4 CD14+4 CCR4+3 CD56+3 CD38+2 CD45RA+2 CXCR3+2 CD33+2 CD28+2 CD27+2 CD3+2
Macrophage   MC22 (3.02%)

▲CD45+10 CD32+10 HLA-DR+8 CD45RO+8 CD44+7 CD69+6 CD64+5 CD14+5 CCR4+4 CXCR3+3 CD33+3 CD28+3 CD56+3 CD11b+3 CD4+2 CD20+2 CD8+2 CD3+2 CD57+2
Macrophage   MC29 (3.06%)

▲CD45+9 CD45RO+7 CD44+6 CD3+6 CD69+5 CD4+3 CD28+3 CD32+3 HLA-DR+3 CD11b+2 CCR4+2 CD43+2 CD14+2 CD27+2 CD8+2 PD-1+2 PD-L1+2
CD4 T cell   MC2b (2.36%)

▲CD45+8 CD32+6 HLA-DR+5 CCR4+4 CD45RO+4 CD44+4 CD64+3 CXCR3+3 CD56+3 CD4+2 CD38+2 TCRγδ+2 CD69+2 CD27+2 CD3+2 CD57+2
Macrophage   MC9 (2.52%)

▲CD45+8 CD32+7 HLA-DR+6 CD64+5 CD45RO+5 CD44+5 CD69+4 CD56+4 CCR4+3 CD57+3 CD38+2 CD14+2 TCRγδ+2 CXCR3+2 CD16+2 CD27+2 CD3+2
Macrophage   MC16 (4.03%)

▲CD45+9 CD32+8 HLA-DR+7 CD45RO+6 CD44+6 CD64+5 CD56+5 CCR4+4 CD14+4 CD69+4 CD57+4 CXCR3+3 TIM3+2 CD11b+2 CD20+2 CD45RA+2 CD33+2 CD27+2 CD8+2
Macrophage   MC23 (4.53%)

▲CD45+10 CD32+9 HLA-DR+8 CD45RO+7 CD44+7 CD64+6 CCR4+5 CD14+5 CD69+5 CD56+5 CXCR3+4 CD57+4 CD11b+3 CD33+3 TIM3+2 CD43+2 CD28+2 CD27+2 CD8+2 PD-1+2
Macrophage   MC30 (3.91%)

▲CD45+6 CD44+6 CD32+4 HLA-DR+4 CD45RO+4 CD16+4 CCR4+3 CXCR3+3 CD56+3 CD19+2 CD64+2 CD14+2 CD69+2 CD8+2 CD57+2 PD-1+2 PD-L1+2
NK cell   MC3 (1.90%)

▲CD45+6 CD44+6 CD32+5 CD56+5 CCR4+4 CD57+4 CD64+4 HLA-DR+3 CD4+2 CD38+2 CXCR3+2 CD28+2 CD45RO+2 CD3+2
Microglia   MC10 (4.77%)

▲CD45+6 CD44+6 CD56+6 CCR4+5 CD32+5 CD57+5 CD64+4 HLA-DR+4 CXCR3+3 CD45RO+3 CD11b+2 CD20+2 CD33+2 CD69+2 CD16+2 PD-1+2 PD-L1+2
Microglia   MC17 (3.79%)

▲CD45+7 CD44+7 CD56+7 CCR4+6 CXCR3+5 CD45RO+4 CD19+2 TIM3+2 CD11b+2 CD20+2 CD43+2 CD14+2 TCRγδ+2 CD33+2 CD69+2 CD16+2 CD8+2 PD-L1+2
Microglia   MC24 (2.93%)

▲CD44+9 CD45+8 CD32+7 CD57+7 CD56+7 HLA-DR+6 CD64+5 CCR4+5 CXCR3+5 CD45RO+5 CD69+4 CD27+3 PD-L1+3 ICOS+2 TIM3+2 CD11b+2 CD4+2 CD38+2 CD43+2 CD14+2 CD45RA+2 CD16+2 CXCR5+2
Microglia   MC31 (3.39%)

▲CD45+6 CD44+5 CD32+4 CD56+4 CCR4+3 CXCR3+3 HLA-DR+3 CD57+3 CD64+2 CD28+2 CD45RO+2 CD16+2 PD-L1+2
Microglia   MC4 (3.60%)

▲CD45+8 CD32+7 CD45RO+6 CD44+6 HLA-DR+4 CD11b+3 CD14+3 CD4+2 CD64+2 CD38+2 CCR4+2 CD33+2 CD69+2 CD16+2 CD8+2 CD3+2 PD-L1+2 CD56+2
Macrophage   MC11 (2.95%)

▲CD45+7 CD32+7 CD44+6 HLA-DR+5 CD45RO+5 CCR4+4 CXCR3+4 CD56+4 CD64+3 CD69+3 CD57+3 CD19+2 CD11b+2 CD20+2 TCRγδ+2 CD8+2
Macrophage   MC18 (2.53%)

▲CD32+10 CD45+9 CD45RO+8 HLA-DR+7 CD44+6 CD64+5 CD69+5 CCR4+4 CD14+4 CD56+4 CXCR3+3 CD11b+2 CD20+2 CD33+2 CD28+2 CD8+2 CD3+2 CD57+2
Macrophage   MC25 (3.01%)

▲CD45+6 CD44+4 CD56+4 CCR4+3 CD32+3 CD57+3 CD4+2 CD64+2 CD69+2 HLA-DR+2
Microglia   MC5 (4.65%)

▲CD45+7 CD32+6 HLA-DR+5 CD45RO+4 CD64+3 CD44+3 CCR4+2 CD14+2 CD69+2 CD16+2 PD-L1+2 CD56+2
Macrophage   MC12 (2.87%)

▲CD56+8 CD44+7 CD57+7 CD45+6 CD32+5 CD64+4 CCR4+4 HLA-DR+4 CXCR3+3 CD45RO+3 PD-L1+3 CD11b+2 CD20+2 TCRγδ+2 CD33+2 CD69+2 CD16+2 CD8+2
Microglia   MC19 (3.84%)

▲CD45+8 CD32+7 HLA-DR+6 CD44+6 CD56+6 CD45RO+5 CD57+5 CD64+4 CCR4+4 CD14+3 CXCR3+3 CD69+3 TIM3+2 CD11b+2 CD4+2 CD20+2 CD43+2 CD8+2 PD-1+2 PD-L1+2
Macrophage   MC26 (0.88%)

▲CD45+6 CD56+6 CD44+5 CD57+5 CD64+3 CCR4+3 CD32+3 HLA-DR+3 CD4+2 CD38+2 CXCR3+2 CD45RO+2 CD27+2 CD3+2
Microglia   MC6 (3.86%)

▲CD56+7 CD45+6 CD44+6 CD57+6 CD32+5 CCR4+4 HLADR+4 CD64+3 CXCR3+3 CD4+2 CD38+2 CD28+2 CD45RO+2 CD27+2 CD3+2 PD-1+2 PD-L1+2
Microglia   MC13 (5.12%)

▲CD45+7 CD44+7 CD32+6 CD56+6 CCR4+5 CXCR3+5 HLA-DR+5 PD-L1+3 TIM3+2 CD11b+2 CD20+2 CD43+2 TCRγδ+2 CD69+2 CD3+2 PD-1+2
Microglia   MC20 (3.31%)

▲CD45+7 CD44+7 CCR4+6 CD32+6 CD56+6 CD64+5 CXCR3+5 HLA-DR+5 CD57+5 CD45RO+4 TIM3+3 CD11b+3 CD43+3 CD69+3 CD4+2 CD38+2 CD14+2 CD8+2 CD3+2 PD-L1+2
Microglia   MC27 (2.99%)

Supplementary Figure 6: Optimization of FlowSOM clustering on t-SNE axes. A) Representative plots demonstrating minimization of the aggregate arcsinh transformed coefficients of variation (left), arcsinh transformed variances (middle), or raw variance (right) for each marker across multiple iterations of FlowSOM clustering. B) Representative heatmap of the arcsinh transformed median mass intensity (left) or interquartile range (IQR) (right) of each indicated marker across each FlowSOM cluster. Colored boxes in the left indicate Citrus identity. Colored boxes on the right indicate an expert-defined immune identify for each cluster. C) Representative assignment of patient-specific cells from Citrus clusters onto t-SNE axes including cell density (far left), enumeration of FlowSOM clusters on the t-SNE axes (mid left), overlay of Citrus populations on to the t-SNE plot (mid right) and assignment of Citrus populations for FlowSOM clusters from which they putatively were down sampled D) Comparison of the frequency of each Citrus cluster identified in each patient to the frequency of the FlowSOM cluster when accurately assigned on the t-SNE space. E) The number of optimized FlowSOM clusters per patient (left), total number of FlowSOM clusters containing cells from Citrus analysis (mid), and proportion of FlowSOM clusters containing Citrus cells was calculated. Significance was determined using a Student's T test. F) Representative MEM labels generated for each patient-specific FlowSOM cluster. Clusters were assigned labels based on marker expression and were color-coded to indicate clusters derived from Citrus. The frequency of each cluster is also indicated. Data in A-C and F represent 1/19 patients included in the Citrus analysis. Data in D and E are generated from 19/19 patients included in the Citrus Analysis.

Supplementary Figure 7

A

LC-03

▲CD44[+7] CD56[+6] CD45[+5] CD45RO[+5] CD57[+5] CCR4[+4] CXCR3[+4] CD28[+4] CD32[+4] CD69[+4] PD-1[+4] PD-L1[+4] CD38[+3] TCRγδ[+3] HLA-DR[+3] CD3[+3] CD19[+2] CD11b[+2] CD64[+2] CD20[+2] CD43[+2] CD45RA[+2] CD33[+2] CD16[+2] CD27[+2] CD8[+2] CXCR5[+2]
Microglia MC1 (5.10%)

▲CD45[+10] CD45RO[+7] CD4[+6] CD44[+6] CD69[+5] CD3[+5] CD57[+5] HLA-DR[+4] CD19[+3] TIM3[+3] CD64[+3] CD43[+3] CD14[+3] TCRγδ[+3] CD28[+3] CD32[+3] CD16[+3] PD-1[+3] PD-L1[+3] CD11b[+2] CD20[+2] CCR4[+2] CD45RA[+2] CXCR3[+2] CD33[+2] CD8[+2] CD56[+2]
CD4 T cell MC4b (2.49%)

▲CD44[+7] CD32[+6] HLA-DR[+6] CD64[+5] CD45[+5] CD57[+5] CD69[+3] CD27[+3] PD-L1[+3] CD56[+3] CXCR3[+3] CD69[+3] CD27[+3] PD-L1[+3] CD56[+3] CD11b[+2] CD4[+2] CCR4[+2] CD43[+2] TCRγδ[+2] CD33[+2] CD28[+2] CD16[+2] CD3[+2] PD-1[+2]
Macrophage MC10 (5.24%)

▲CD45[+8] CD64[+7] CD32[+7] HLA-DR[+6] CD69[+4] CD45RO[+4] TIM3[+3] CD11b[+3] CD38[+3] CCR4[+3] CD3[+3] CD19[+2] CD4[+2] CD14[+2] TCRγδ[+2] CD33[+2] CD28[+2]
Macrophage MC15b (3.62%)

▲CD45[+10] CD45RO[+6] CD44[+6] CD69[+5] CD8[+5] CD3[+5] HLA-DR[+4] CD43[+3] TCRγδ[+3] CD33[+3] PD-1[+3] CD20[+3] CCR4[+2] CXCR3[+2] CD28[+2] CD32[+2] CD27[+2] CD57[+2]
CD8 T cell MC2a (4.08%)

▲CD56[+7] HLA-DR[+6] CD44[+6] CD57[+6] CD45[+5] CD32[+4] CD4[+3] CD64[+3] CD45RO[+3] CD16[+3] CD3[+3] CXCR5[+3] PD-1[+3] CD11b[+2] CXCR3[+2] CD69[+2] CD27[+2]
Microglia MC5 (6.44%)

▲CD45[+7] CD32[+7] HLA-DR[+6] CD45RO[+6] CD64[+5] CD44[+5] CCR4[+4] CD20[+3] CXCR3[+3] CD33[+3] CD69[+3] CD8[+3] PD-1[+3] CD19[+2] CD11b[+2] CD4[+2] CD43[+2] CD14[+2] TCRγδ[+2] CD45RA[+2] CD28[+2] CD16[+2] CD27[+2] CD57[+2]
Macrophage MC11 (4.82%)

▲CD45[+9] CD32[+9] CD64[+8] HLA-DR[+8] CD45RO[+8] CD69[+6] CD44[+6] CD11b[+4] CD14[+4] CD33[+4] CD19[+3] TIM3[+3] CD4[+3] CD20[+3] CD28[+3] CD16[+3] CD38[+2] CCR4[+2] CD43[+2] TCRγδ[+2] CD45RA[+2] CXCR3[+2] CD3[+2]
Macrophage MC16 (8.84%)

▲CD45[+9] CD45RA[+7] CD64[+3] CD43[+3] CD33[+3] CD28[+3] CD45RO[+3] CD44[+3] CD27[+3] CD11b[+2] CD38[+2] TCRγδ[+2] CXCR3[+2] CD3[+2]
γδ T cell MC2b (0.99%)

▲CD69[+5] CD16[+5] CD3[+5] CD19[+4] TIM3[+4] CD43[+4] CD45RA[+4] CD45[+4] CD28[+4] CD45RO[+4] PD-1[+4] ICOS[+3] CD11b[+3] CD64[+3] CD20[+3] CD14[+3] TCRγδ[+3] CXCR3[+3] CD33[+3] CD27[+3] CD57[+3] CD56[+3] CD4[+2] HLA-DR[+2] CD8[+2]
NK cell MC6 (0.09%)

▲CD32[+6] HLA-DR[+6] CD64[+5] CD45[+5] CD69[+4] CD45RO[+4] ICOS[+3] CCR4[+3] TCRγδ[+3] CD45RA[+3] CXCR3[+3] CD16[+3] CD57[+3] PD-1[+3] CD11b[+2] CD4[+2] CD20[+2] CD14[+2] CD33[+2] CD28[+2] CD44[+2] CD3[+2] CD56[+2]
Microglia MC12 (0.48%)

▲CD45[+10] CD32[+9] HLA-DR[+8] CD45RO[+8] CD64[+7] CD44[+7] CD69[+6] CD11b[+5] CD14[+5] CD33[+5] CD4[+4] TCRγδ[+3] CD28[+3] CD8[+3] CD19[+2] CD20[+2] CD38[+2] CD43[+2] CD45RA[+2] CD16[+2] CD3[+2]
Macrophage MC17 (5.79%)

▲CD45[+9] CD45RO[+6] CD44[+5] CD8[+5] CD3[+5] CD69[+4] CD57[+4] CD19[+3] CD11b[+3] CD43[+3] CD14[+3] TCRγδ[+3] CD33[+3] HLA-DR[+3] PD-1[+3] CD20[+2] CCR4[+2] CD32[+2] CD56[+2]
CD8 T cell MC2c (2.70%)

▲CD45[+5] CD32[+4] HLA-DR[+4] CD64[+3] CCR4[+3] TCRγδ[+3] CD45RO[+3] CD14[+2] CXCR3[+2] CD28[+2] CD69[+2] CD16[+2] CD56[+2]
Microglia MC7 (6.87%)

▲CD45[+7] CD32[+7] CD64[+6] CCR4[+6] HLA-DR[+6] CD45RO[+6] CD69[+4] CD20[+3] CXCR3[+3] CD44[+3] CD27[+3] PD-1[+3] CD19[+2] CD11b[+2] CD4[+2] CD43[+2] CD14[+2] TCRγδ[+2] CD33[+2] CD28[+2] PD-L1[+2]
Macrophage MC13 (4.64%)

▲CD45[+8] CD64[+7] CD32[+7] HLA-DR[+7] CD45RO[+5] CD69[+4] CD57[+4] CD11b[+3] CD14[+3] CD45RA[+3] CD33[+3] CD16[+3] CD3[+3] PD-1[+3] PD-L1[+3] CD19[+2] TIM3[+2] CD4[+2] CXCR3[+2] CD28[+2] CD56[+2]
Macrophage MC18 (3.00%)

▲CD57[+5] CD45[+4] HLA-DR[+3] CD56[+3] CD11b[+2] CD43[+2] CD33[+2] CD32[+2] CD45RO[+2] CD44[+2] CD3[+2] PD-L1[+2]
Microglia MC3 (6.51%)

▲CD57[+6] CD45[+5] CD32[+5] HLA-DR[+5] CD45RO[+4] CD44[+4] CD19[+3] CD64[+3] CD43[+3] CD3[+3] CD56[+3] CD4[+2] CCR4[+2] CXCR3[+2] CD33[+2] CD69[+2] CD27[+2] PD-1[+2]
Microglia MC8 (2.91%)

▲CD32[+9] CD64[+8] CD45[+8] HLA-DR[+8] CD69[+6] CD45RO[+6] CD44[+6] CD57[+5] CD11b[+4] CD14[+4] CD33[+4] CD4[+3] CD20[+3] CD28[+3] CD8[+3] TIM3[+3] CD43[+2] TCRγδ[+2] CD45RA[+2] CXCR3[+2] CD16[+2] CD3[+2] PD-1[+2] CD56[+2]
Macrophage MC14 (4.22%)

▲CD45[+8] CD64[+7] CD32[+7] HLA-DR[+7] CD45RO[+6] CD69[+4] CD44[+4] CD19[+3] CD11b[+3] CD14[+3] CD45RA[+3] CD33[+3] CD16[+3] CD27[+3] CD3[+3] CD4[+2] CD38[+2] CCR4[+2] CD43[+2] TCRγδ[+2] CD28[+2]
Macrophage MC19 (8.79%)

▲CD45[+10] CD45RO[+8] CD4[+7] CD44[+6] CD69[+5] CD3[+5] CD28[+4] HLA-DR[+4] CD19[+3] TIM3[+3] CD64[+3] CD43[+3] CD14[+3] TCRγδ[+3] CD33[+3] CD32[+3] CD16[+3] CD57[+3] PD-1[+3] CD11b[+2] CD20[+2] CD38[+2] CCR4[+2] CD45RA[+2] CXCR3[+2] CD27[+2] CD8[+2]
CD4 T cell MC4a (4.74%)

▲CD64[+5] CD45[+5] CD32[+5] HLA-DR[+5] CD45RO[+4] CCR4[+3] CXCR3[+3] CD69[+3] CD44[+3] CD8[+3] PD-1[+3] PD-L1[+3] CD19[+2] CD11b[+2] TCRγδ[+2] CD33[+2] CD28[+2] CD16[+2] CD27[+2] CD57[+2] CD56[+2]
Microglia MC9 (3.32%)

▲CD45[+9] CD64[+8] CD32[+7] HLA-DR[+7] CD69[+6] CD45RO[+6] CD33[+4] CD57[+3] CD43[+3] CD20[+3] CD14[+3] CD45RA[+3] CD16[+3] CD3[+3] PD-L1[+3] CD19[+2] TIM3[+2] CD38[+2] CCR4[+2] TCRγδ[+2] CXCR3[+2] CD28[+2] CD44[+2] CD57[+2]
Macrophage MC15a (4.52%)

B

LC-06

▲CD45[+9] TCRγδ[+2]
γδ T cells MC1 (9.69%)

▲CD45[+8]
DN T cells MC7 (9.57%)

▲CD45[+6] CD45RO[+5] CD11b[+4] CD32[+3] CD44[+3]
Microglia MC13 (1.87%)

▲CD45[+6] CD28[+5] CD32[+5] HLA-DR[+5] CD64[+4] CXCR3[+4] CD33[+4] CD45RO[+2]
Microglia MC19 (2.77%)

▲CD45[+6] CD28[+2]
B cells MC2 (0.15%)

▲CD45[+6] CD45RA[+4] CD44[+3] CD43[+2]
B cells MC8 (3.87%)

▲CD45[+5] CD44[+4] HLA-DR[+3] CD45RO[+3] CD32[+2] PD-L1[+2]
Microglia MC14 (3.99%)

▲CD45[+6] CD64[+5] HLA-DR[+5] CCR4[+3] CXCR3[+3] CD32[+3] CD45RO[+3] PD-L1[+3] CD69[+2]
Microglia MC20 (7.15%)

▲CD45[+9] CD45RA[+8] CD16[+5] CD43[+4] CD44[+3]
NK cells MC3 (2.37%)

▲CD45[+6] CD44[+3] CD3[+3] CD43[+2] CD45RA[+2]
DN T cells MC9 (3.37%)

▲CD45[+5] CD44[+4] HLA-DR[+4] CXCR3[+3] CD32[+3] CD45RO[+3] PD-L1[+3] CD11b[+2] CD64[+2] CCR4[+2]
Microglia MC15 (3.49%)

▲CD45[+6] CD64[+5] CD32[+4] HLA-DR[+4] CD45RO[+4]
Microglia MC21 (4.78%)

▲CD45[+10] CD45RA[+6] CD44[+5] CD43[+4] CD3[+4] CD8[+2]
CD8 T cells MC4 (3.39%)

▲CD45[+7] CD45RO[+5] CD44[+4] CD3[+3]
DN T cells MC10 (4.93%)

▲CD45[+5] CD64[+4] CD32[+3] HLA-DR[+3] CD45RO[+3] PD-L1[+3] CD11b[+2] CCR4[+2] CXCR3[+2] CD44[+2]
Microglia MC16 (3.79%)

▲CD45[+7] HLA-DR[+6] CD64[+5] CD32[+5] CD45RO[+4] CD44[+3] CD57[+3] CD11b[+2] CD69[+2]
Microglia MC22 (2.02%)

▲CD45[+10] CD45RO[+7] CD44[+5] CD43[+3] CD3[+3] CD8[+2]
CD8 T cells MC5 (3.62%)

▲CD45[+9] CD45RO[+6] CD44[+6] CD3[+4] CCR4[+3] CD43[+3] CD27[+3] CXCR3[+2] CD28[+2] HLA-DR[+2] CD16[+2] CD8[+2] PD-1[+2]
CD8 T cells MC11 (0.06%)

▲CD45[+5] CD64[+4] CD32[+3] HLA-DR[+3] CD45RO[+3]
Microglia MC17 (9.34%)

▲CD64[+6] CD45[+6] HLA-DR[+5] CD32[+4] CD45RO[+4] CD11b[+2] CCR4[+2] CXCR3[+2] CD69[+2] CD57[+2] PD-L1[+2]
Microglia MC23 (5.59%)

▲CD45[+10] CD45RO[+7] CD44[+5] CD4[+4] CD43[+3] CD3[+3]
CD4 T cells MC6 (7.97%)

▲TIM3[+8] CD45[+8] CD19[+2] CD11b[+2]
B cell MC12 (0.10%)

▲CD45[+6] HLA-DR[+4] CD64[+3] CCR4[+2] CXCR3[+2] CD32[+2] CD45RO[+2] PD-L1[+2]
Microglia MC18 (4.01%)

▲CD45[+7] CD64[+6] HLA-DR[+5] CD45RO[+5] CCR4[+4] CXCR3[+4] CD32[+4] PD-L1[+4] CD11b[+2] CD69[+2] CD44[+2]
Microglia MC24 (2.10%)

Supplementary Figure 7: Individual patient MEM labels for each FlowSOM Cluster. A) MEM labels were generated for each of 19 FlowSOM clusters (MC) identified in patient LC-03. B) MEM labels generated for each of 24 FlowSOM clusters (MC) identified in patient LC-06. Each label is color coded to its corresponding Citrus identity. Percentages in parentheses indicate the frequency of each cluster within the CD45+ fraction in each patient.
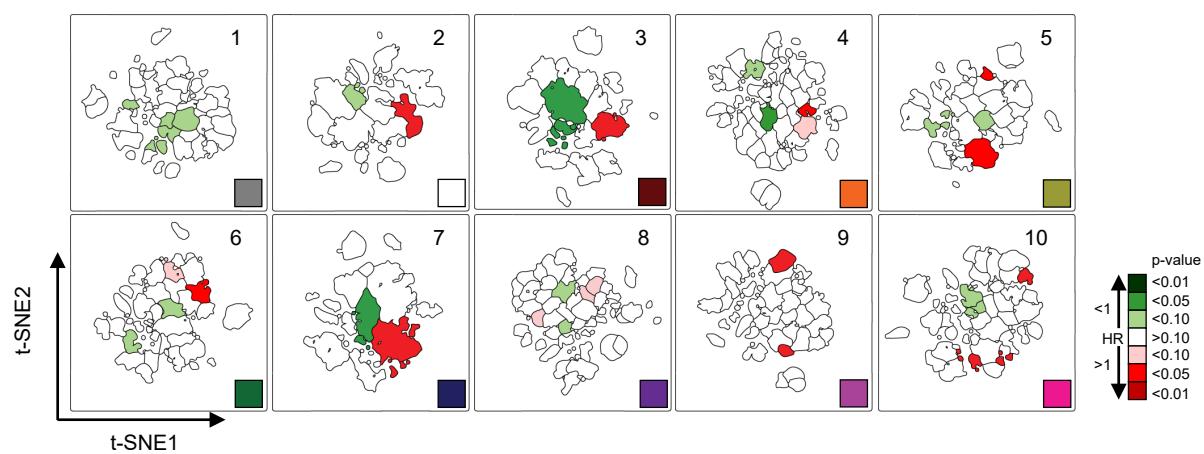
Supplementary Figure 8
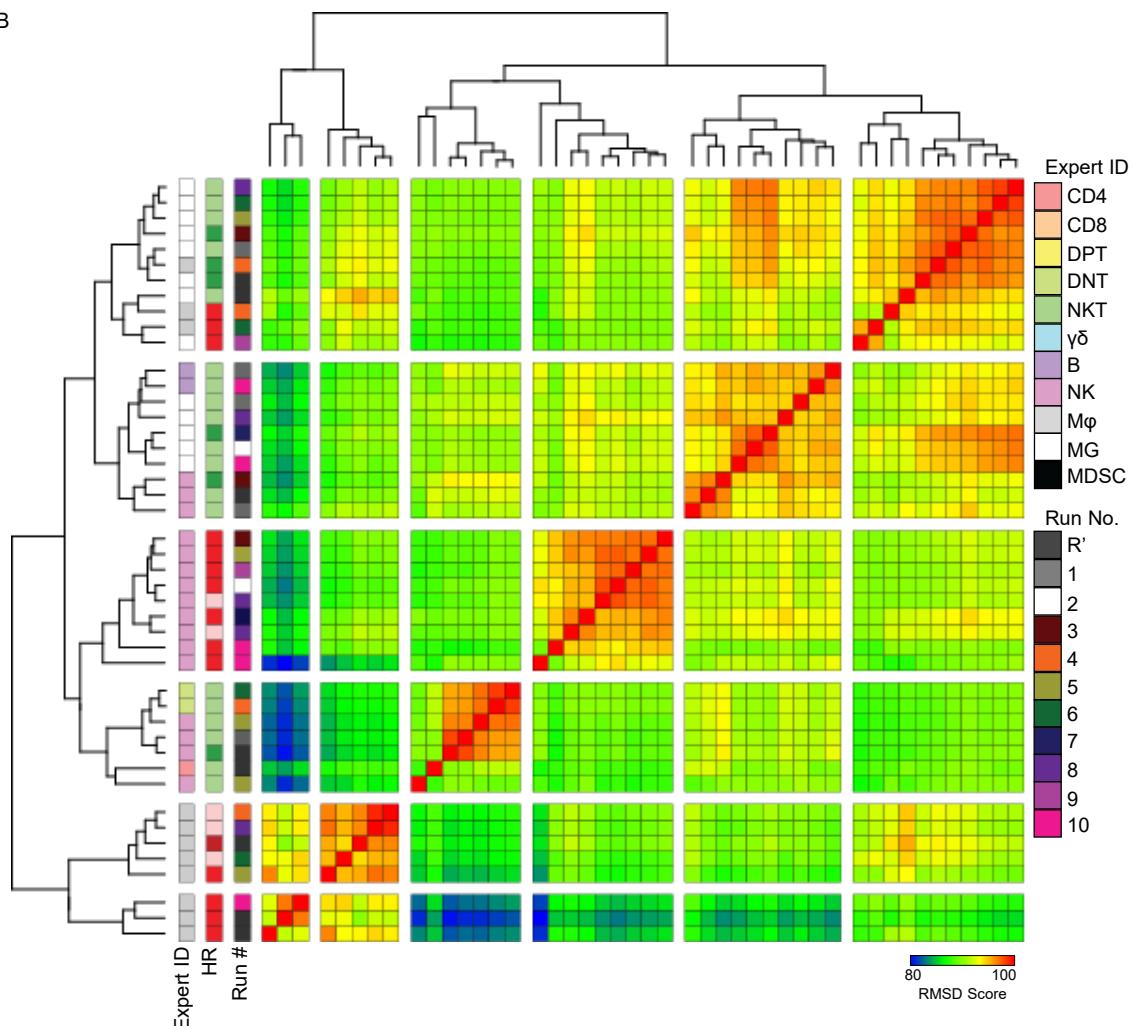
Supplementary Figure 8: RMSD registration of FlowSOM clusters. A) Root mean squared deviation (RMSD) was performed to compare the phenotypic similarities between 455 FlowSOM clusters across 19/32 GBM patients, identifying 17 common immune phenotypes. B) Graph indicating the number of patients represented within each RMSD metacluster. C) Pie charts indicate the proportion of FlowSOM clusters derived from each patient within each indicated RMSD metacluster. D) Bar chart indicating the percentage of FlowSOM clusters derived from C-GBM or NC-GBM patients within each RMSD metacluster. E) MEM labels from pooled FlowSOM clusters indicate the cellular phenotypes of each larger RMSD metacluster. Red= C-GBM. Blue= NC-GBM. A Chi-Squared analysis determined statistical enrichment. * = p<0.05, ** = p<0.01, *** = p<0.001, **** = p <0.0001.

Supplementary Figure 9

A

B
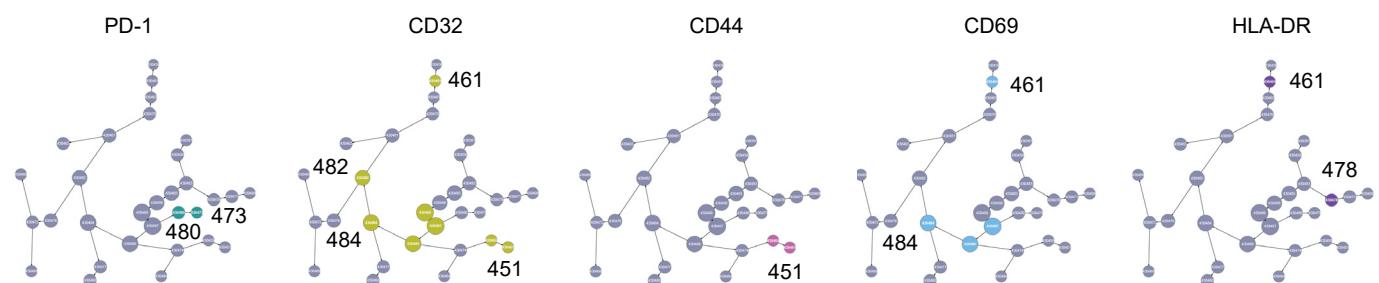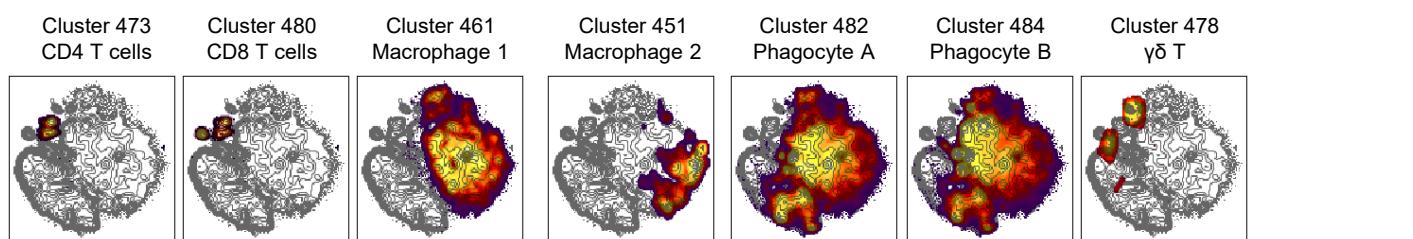
Supplementary Figure 9: Outcome stratifying immune populations are stably detected by RAPID. A) t-SNE maps indicating FlowSOM clusters whose abundance stratify patient outcome as identified in 10 different implementations of the RAPID algorithm randomly subsampling cells from n=19/32 GBM patients. B) RMSD was performed to compare the phenotypic similarities between all risk-stratifying immune populations identified by RAPID. Colors in A indicate the hazard associated with more (green) or less (red) favorable outcomes. Colored boxes in B indicate the expert identification for each immune subset, hazard ratio, or RAPID iteration respectively.

Supplementary Figure 10

A

PD-1   CD32   CD44   CD69   HLA-DR

B

Cluster 473   Cluster 480   Cluster 461   Cluster 451   Cluster 482   Cluster 484   Cluster 478
CD4 T cells   CD8 T cells   Macrophage 1   Macrophage 2   Phagocyte A   Phagocyte B   γδ T
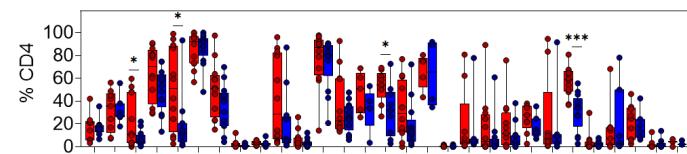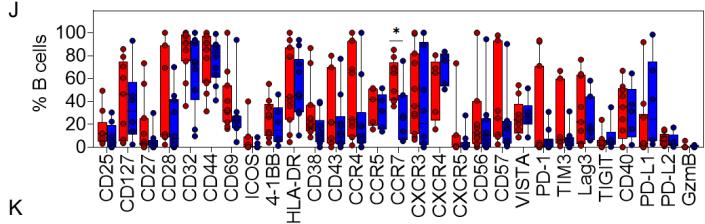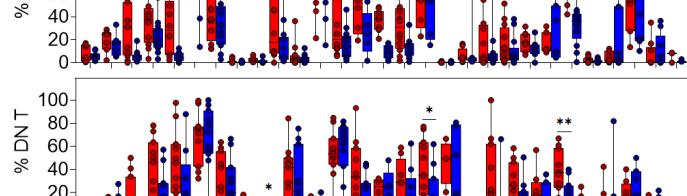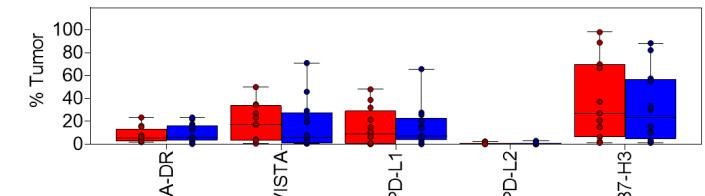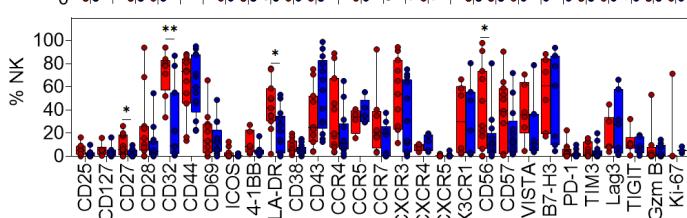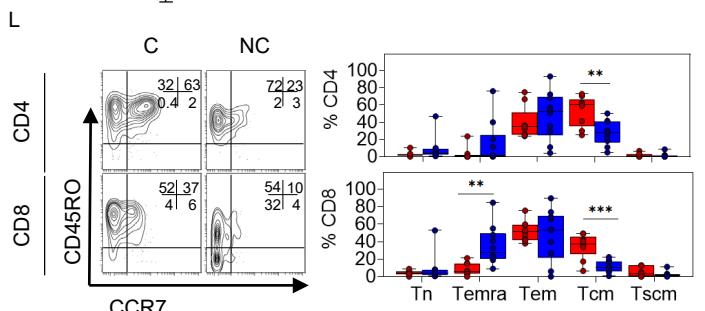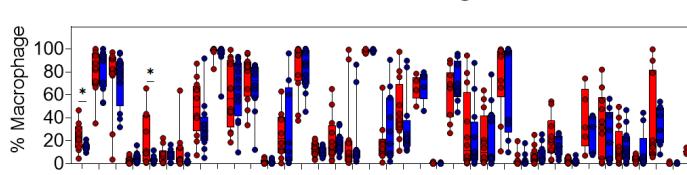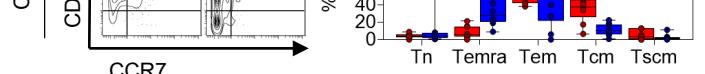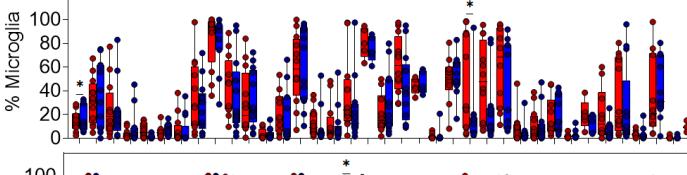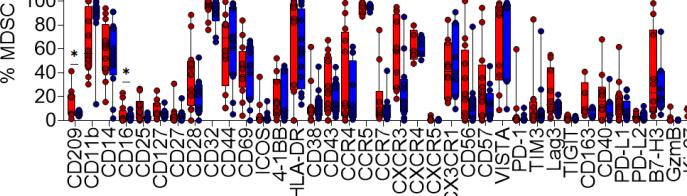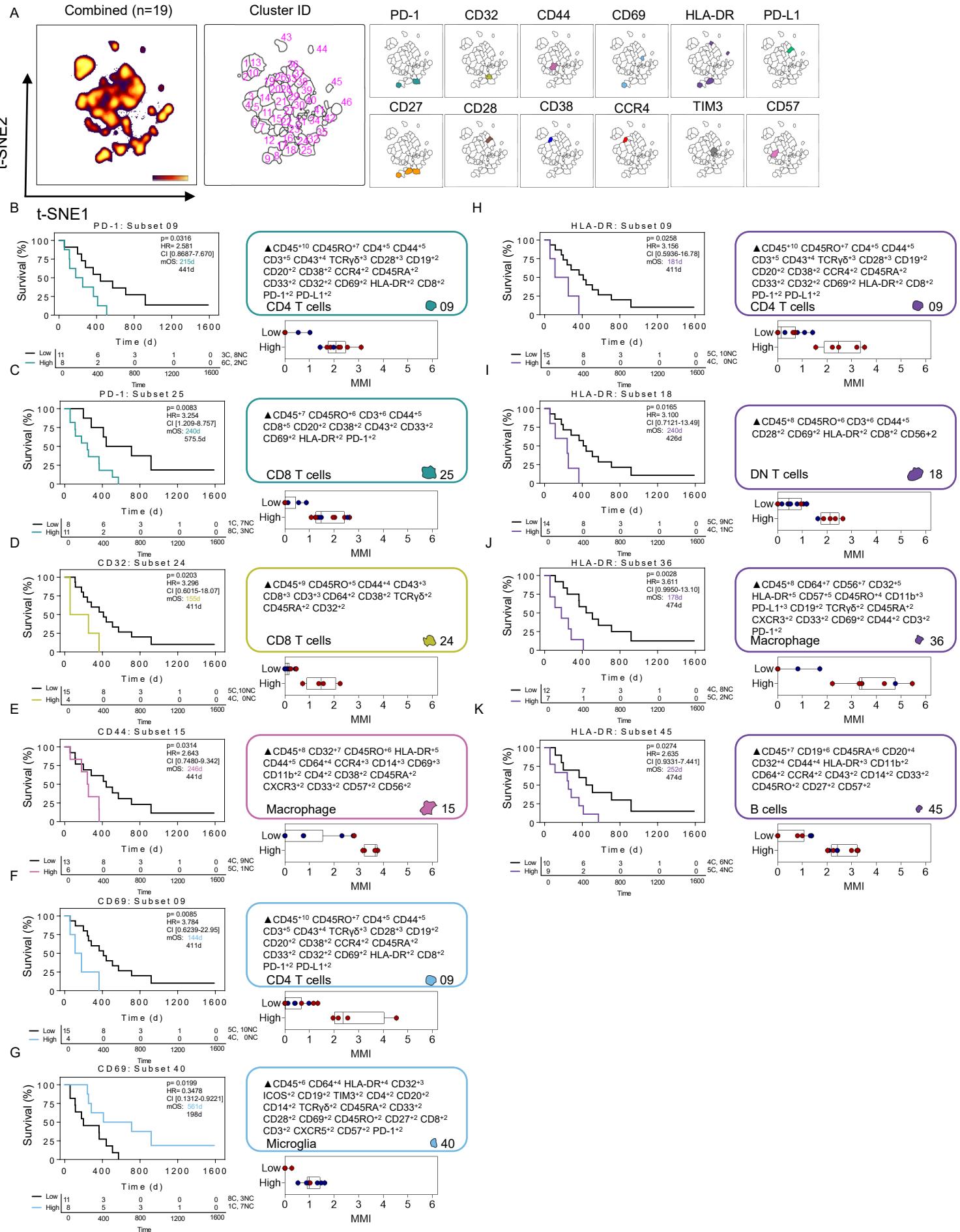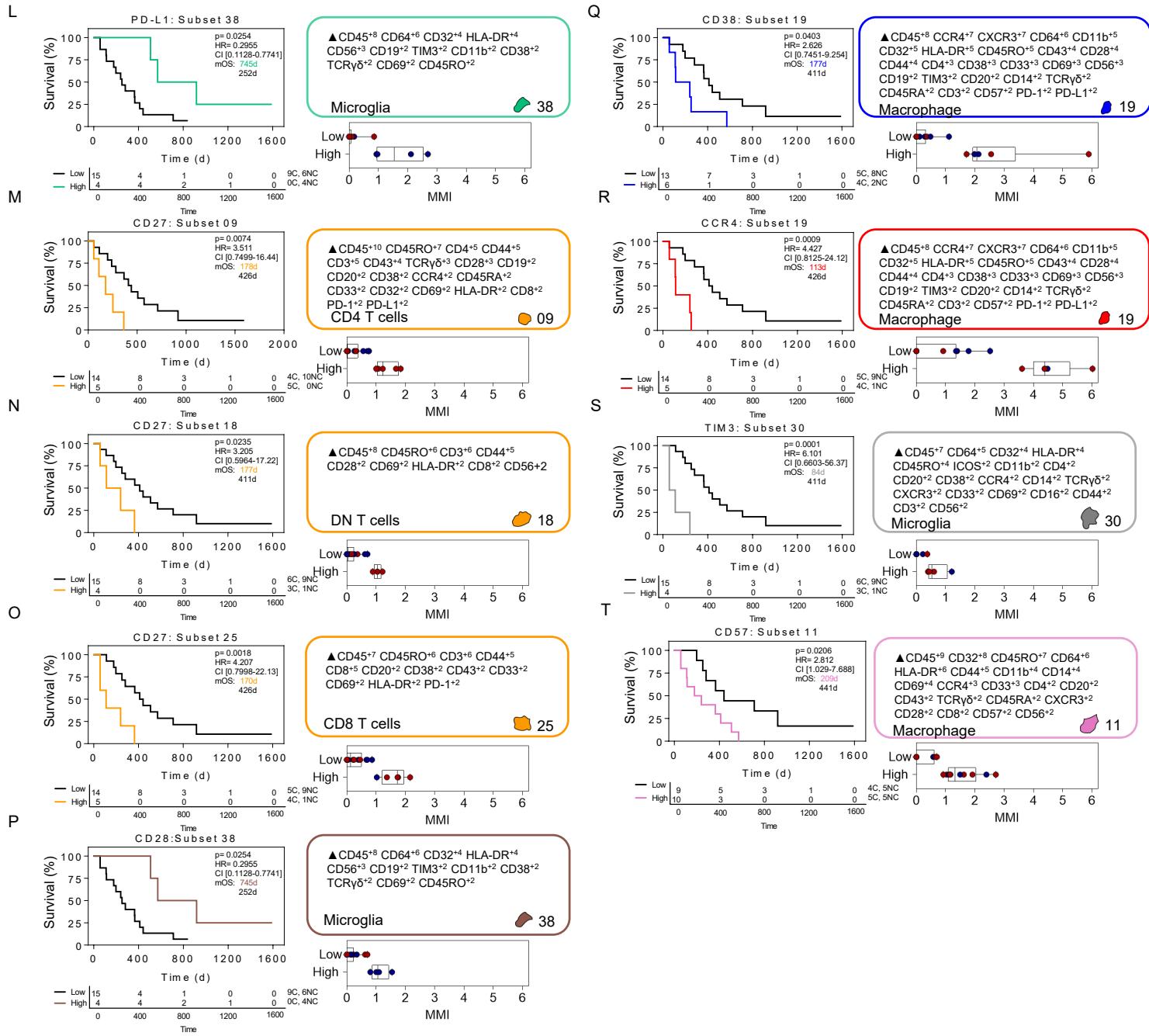
Supplementary Figure 10: Immune cell phenotypes associated with tumor contact with the lateral ventricle. A) Citrus clustergrams of immune clusters with statistically different expression of the indicated marker. The most terminal clusters where indicated were chosen for further analysis. B) Representative overlay of indicated Citrus clusters (heat) onto the t-SNE map (contour). C-K) Box and whisker plots indicating the frequency (median ± IQR) of CD4 T cells (C), CD8 T cells (D), DNT cells (E), NK cells (F), macrophages (G), microglia (H), myeloid derived suppressor cells (I) B cells (J) or CD45$^-$ tumor cells (K) expressing each indicated marker. L) Representative biaxial plots defining the frequency of memory T cells subsets in C- and NC-GBM. Box and whisker plots quantifying the frequency of each memory T cell subset. Data in C-K represent n=12 C-GBM and n=13 NC-GBM. Box and whisker plots in L represent n=9 C-GBM and n=10 NC-GBM. Statistical significance was determined using a 2-way ANOVA with Sidak's multiple comparisons test. * = p<0.05, ** = p<0.01, *** = p<0.001, **** = p <0.0001.

Supplementary Figure 11

A Combined (n=19) | Cluster ID | PD-1, CD32, CD44, CD69, HLA-DR, PD-L1, CD27, CD28, CD38, CCR4, TIM3, CD57

B PD-1: Subset 09
p= 0.0316
HR= 2.581
CI [0.8687-7.670]
mOS: 215d
441d
▲CD45+10 CD45RO+7 CD4+5 CD44+5 CD3+5 CD43+4 TCRγδ+3 CD28+3 CD19+2 CD20+2 CD38+2 CCR4+2 CD45RA+2 CD33+2 CD32+2 CD69+2 HLA-DR+2 CD8+2 PD-1+2 PD-L1+2
CD4 T cells 09
Low: 11 6 3 0 0 3C, 8NC
High: 8 2 0 0 0 6C, 2NC

C PD-1: Subset 25
p= 0.0083
HR= 3.254
CI [1.209-8.757]
mOS: 240d
575.5d
▲CD45+7 CD45RO+6 CD3+6 CD44+5 CD8+5 CD20+2 CD38+2 CD43+2 CD33+2 CD69+2 HLA-DR+2 PD-1+2
CD8 T cells 25
Low: 8 6 3 1 0 1C, 7NC
High: 11 2 0 0 0 8C, 3NC

D CD32: Subset 24
p= 0.0203
HR= 3.296
CI [0.6015-18.07]
mOS: 155d
411d
▲CD45+9 CD45RO+5 CD44+4 CD43+3 CD8+3 CD3+3 CD64+2 CD38+2 TCRγδ+2 CD45RA+2 CD32+2
CD8 T cells 24
Low: 15 8 3 1 0 5C, 10NC
High: 4 0 0 0 0 4C, 0NC

E CD44: Subset 15
p= 0.0314
HR= 2.643
CI [0.7480-9.342]
mOS: 246d
441d
▲CD45+8 CD32+7 CD45RO+6 HLA-DR+5 CD44+5 CD64+4 CD4+3 CD14+3 CD69+3 CD11b+2 CD4+2 CD38+2 CD45RA+2 CXCR3+2 CD33+2 CD57+2 CD56+2
Macrophage 15
Low: 13 8 3 1 0 4C, 9NC
High: 6 0 0 0 0 5C, 1NC

F CD69: Subset 09
p= 0.0085
HR= 3.784
CI [0.6239-22.95]
mOS: 144d
411d
▲CD45+10 CD45RO+7 CD4+5 CD44+5 CD3+5 CD43+4 TCRγδ+3 CD28+3 CD19+2 CD20+2 CD38+2 CCR4+2 CD45RA+2 CD33+2 CD32+2 CD69+2 HLA-DR+2 CD8+2 PD-1+2 PD-L1+2
CD4 T cells 09
Low: 15 8 3 1 0 5C, 10NC
High: 4 0 0 0 0 4C, 0NC

G CD69: Subset 40
p= 0.0199
HR= 0.3478
CI [0.1312-0.9221]
mOS: 561d
198d
▲CD45+6 CD64+4 HLA-DR+4 CD32+3 ICOS+2 CD19+2 TIM3+2 CD4+2 CD20+2 CD14+2 TCRγδ+2 CD45RA+2 CD33+2 CD28+2 CD69+2 CD45RO+2 CD27+2 CD8+2 CD3+2 CXCR5+2 CD57+2 PD-1+2
Microglia 40
Low: 11 3 3 0 0 8C, 3NC
High: 8 5 3 1 0 1C, 7NC

H HLA-DR: Subset 09
p= 0.0258
HR= 3.156
CI [0.5936-16.78]
mOS: 181d
411d
▲CD45+10 CD45RO+7 CD4+5 CD44+5 CD3+5 CD43+4 TCRγδ+3 CD28+3 CD19+2 CD20+2 CD38+2 CCR4+2 CD45RA+2 CD33+2 CD32+2 CD69+2 HLA-DR+2 CD8+2 PD-1+2 PD-L1+2
CD4 T cells 09
Low: 15 8 3 1 0 5C, 10NC
High: 4 0 0 0 0 4C, 0NC

I HLA-DR: Subset 18
p= 0.0165
HR= 3.100
CI [0.7121-13.49]
mOS: 240d
426d
▲CD45+8 CD45RO+6 CD3+6 CD44+5 CD28+2 CD69+2 HLA-DR+2 CD8+2 CD56+2
DN T cells 18
Low: 14 8 3 1 0 5C, 9NC
High: 5 0 0 0 0 4C, 1NC

J HLA-DR: Subset 36
p= 0.0028
HR= 3.611
CI [0.9950-13.10]
mOS: 178d
474d
▲CD45+8 CD64+7 CD56+7 CD32+5 HLA-DR+5 CD57+5 CD45RO+4 CD11b+3 PD-L1+3 CD19+2 TCRγδ+2 CD45RA+2 CXCR3+2 CD33+2 CD69+2 CD44+2 CD3+2 PD-1+2
Macrophage 36
Low: 12 7 3 1 0 4C, 8NC
High: 7 1 0 0 0 5C, 2NC

K HLA-DR: Subset 45
p= 0.0274
HR= 2.635
CI [0.9331-7.441]
mOS: 252d
474d
▲CD45+7 CD19+6 CD45RA+6 CD20+4 CD32+4 CD44+4 HLA-DR+3 CD11b+2 CD64+2 CCR4+2 CD43+2 CD14+2 CD33+2 CD45RO+2 CD27+2 CD57+2
B cells 45
Low: 10 6 3 0 0 4C, 6NC
High: 9 2 0 0 0 5C, 4NC

Supplementary Figure 11: Immune receptor expression correlates with patient outcomes. A) t-SNE plots representing CD45+ cells pooled from n=19 GBM patients and enumeration of FlowSOM clusters on the t-SNE axes. Colored clusters indicate clusters identified by mmRAPID for which expression of the indicated markers stratify patient outcomes. B-K) Kaplan-Meier curves indicating overall survival in immune subsets stratifying patient outcome identified by mmRAPID analysis. Calculated MEM labels identified key features of stratifying immune subsets. Box and whisker diagrams plot the arcsinh transformed median mass intensity for PD-1 expression (B, C), CD32 (D), CD44 (E), CD69 (F, G), and HLA-DR (H, I, J, K) in stratified high and low groups. Kaplan-Meier curves indicating overall survival in immune subsets stratifying patient outcome identified by mmRAPID analysis. Calculated MEM labels identified key features of stratifying immune subsets. Box and whisker diagrams plot the arcsinh transformed median mass intensity for PD-L1 expression (L) CD27 (M-O), CD28 (P), CD38 (Q), CCR4 (R), TIM3 (S), and CD57 (T) in stratified high and low groups.

A

IL-2
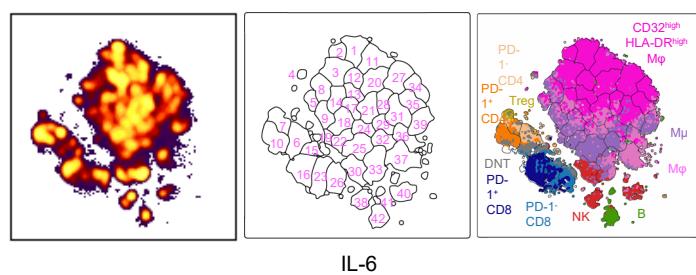
Supplementary Figure 12: Immune induction of protein phosphorylation during IL-2 stimulation. A) Graphs indicating the arcsinh transformed phosphoprotein median intensities for each phosphoprotein in each of 42 IL-2 stimulated immune clusters. Graphs indicate the median ± IQR from 5 C-GBM and 5 NC-GBM patients. Black horizontal lines indicate signaling threshold for each arcsinh transformed value. Black dotted boxes indicate clusters for which the arcsinh transformed median mass intensity surpassed the signaling threshold (±0.2-fold change) in either the C-GBM or NC-GBM cohort. A Student's T test with Bonferroni's correction for multiple comparisons was used to test for statistical significance. * = $p<0.05$, ** = $p<0.01$, *** = $p<0.001$, **** = $p<0.0001$.
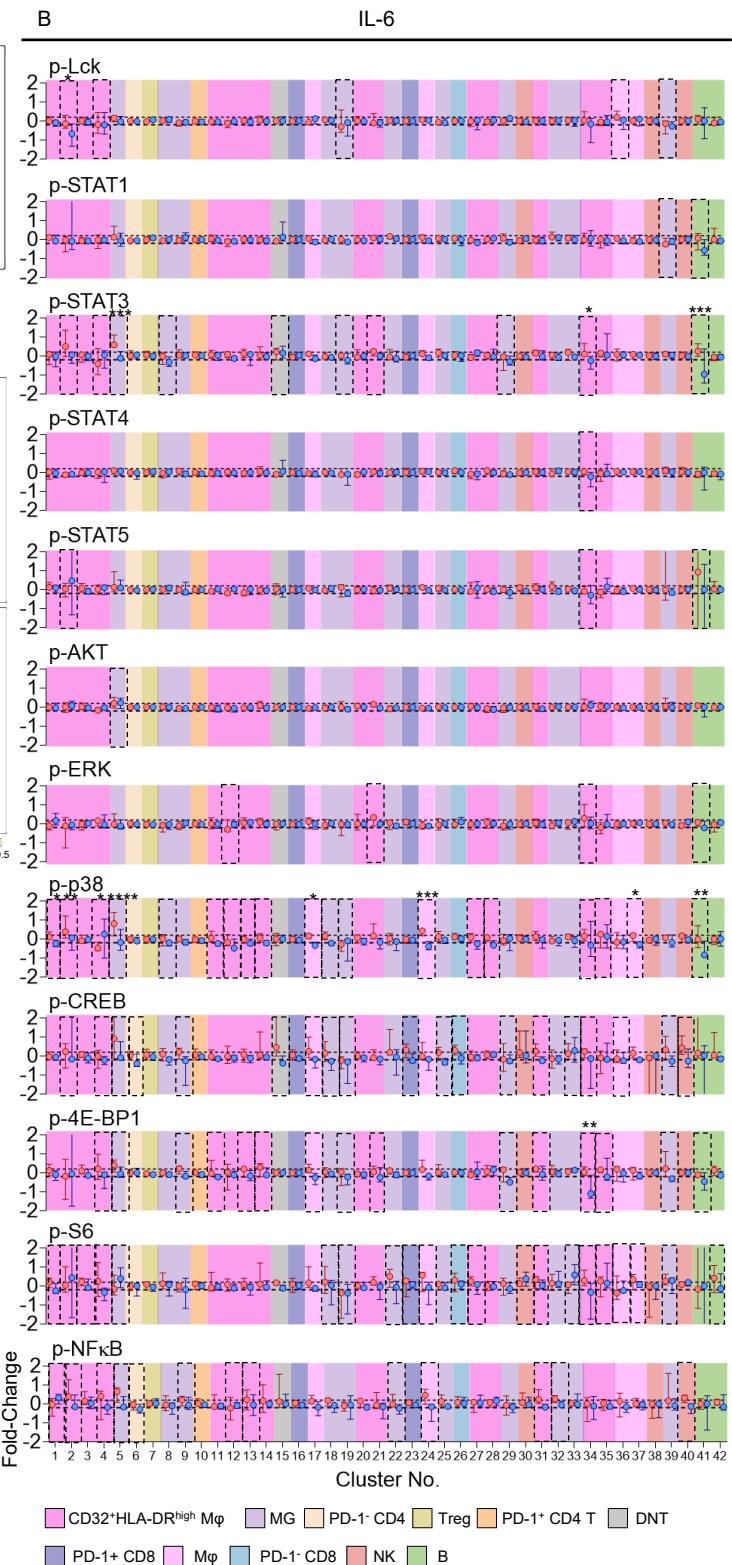
Supplementary Figure 13
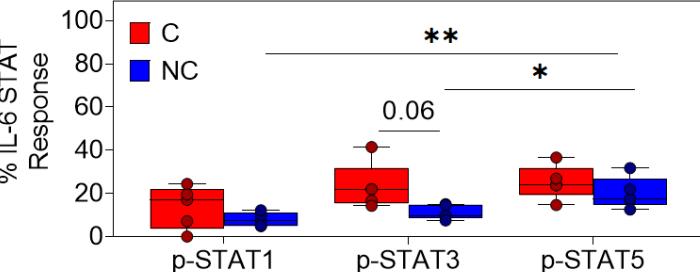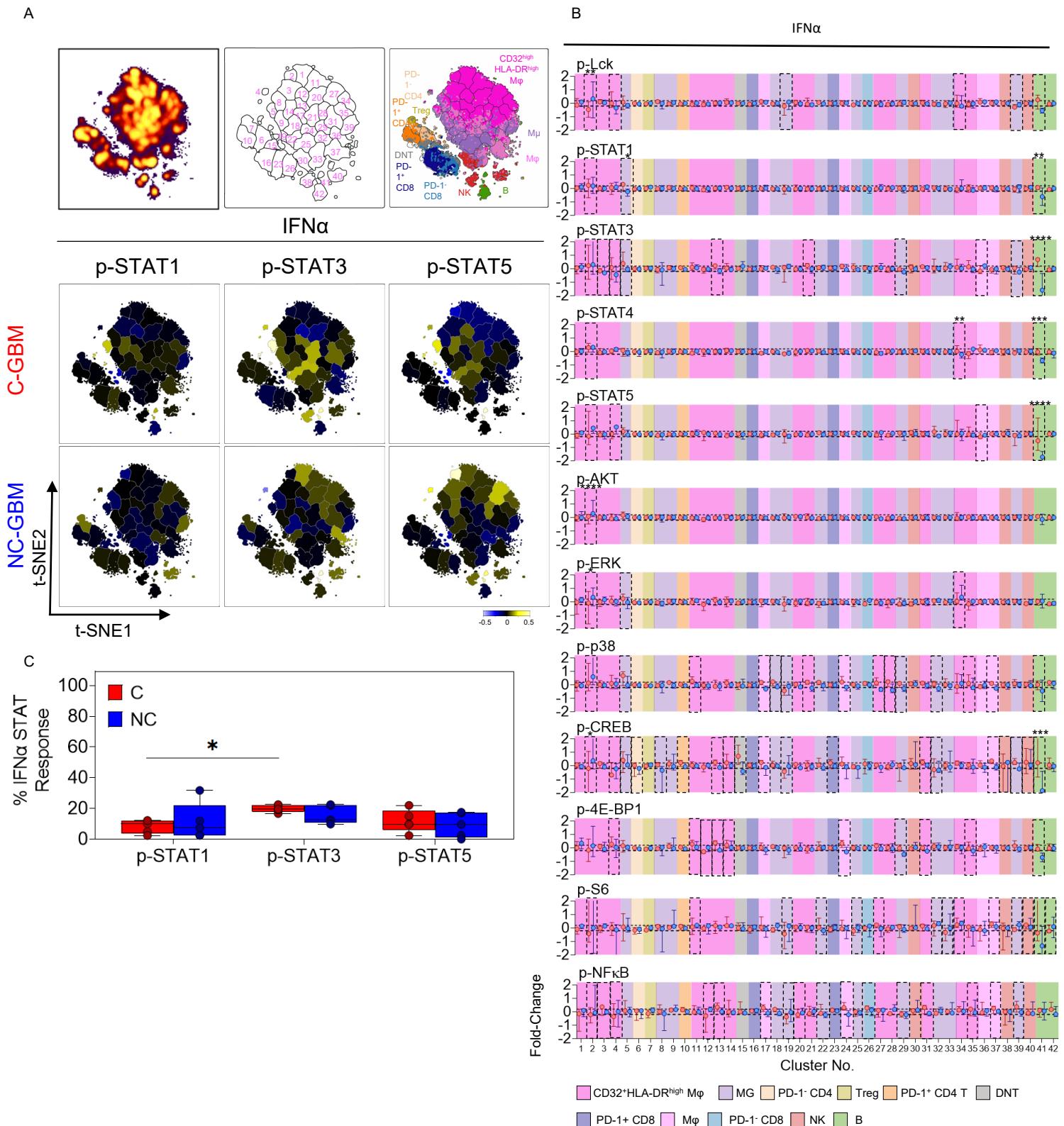
Supplementary Figure 13: Interleukin 6 induces STAT3 and STAT5 signaling in GBM immune infiltrates. A) Representative t-SNE plot indicated the density of CD45+ leukocytes (left), enumerated FlowSOM clusters (middle) and overlay of expertly gated immune populations onto the clustered t-SNE axes (right). Representative heatmaps on the t-SNE axes indicate the cluster-specific median arcsinh-fold change of the indicated phosphoprotein under IL-6 stimulation conditions compared to basal phosphorylation. B) Graphs indicating the arcsinh transformed phosphoprotein median intensities for each phosphoprotein in each of 42 IL-6 stimulated immune clusters. C) Box and whisker plots indicating the proportion of clusters in C-GBM or NC-GBM immune infiltrates surpassing the phospho-signaling threshold (>0.2 arcsinh fold change) in response to IL-6 stimulation. Graphs indicate the median ± IQR. Black horizontal lines in b indicate signaling threshold for each arcsinh transformed value. Black dotted boxes in b indicate clusters for which the arcsinh transformed median mass intensity surpassed the signaling threshold (±0.2-fold change) in either the C-GBM or NC-GBM cohort). A Student's T test with Bonferroni's correction for multiple comparisons was used to test for statistical significance. * = $p<0.05$, ** = $p<0.01$, *** = $p<0.001$, **** = $p <0.0001$.

Supplementary Figure 14: Interferon alpha preferentially induces STAT3 phosphorylation in C-GBM immune infiltrates. A) Representative t-SNE plot indicated the density of CD45+ leukocytes (left), enumerated FlowSOM clusters (middle) and overlay of expertly gated immune populations onto the clustered t-SNE axes (right). Representative heatmaps on the t-SNE axes indicate the cluster-specific median arcsinh-fold change of the indicated phosphoprotein under IFNα stimulation conditions compared to basal phosphorylation. B) Graphs indicating the arcsinh transformed phosphoprotein median intensities for each phosphoprotein in each of 42 IFNα stimulated immune clusters. C) Box and whisker plots indicating the proportion of clusters in C-GBM or NC-GBM immune infiltrates surpassing the phospho-signaling threshold (>0.2 arcsinh fold change) in response to IFNα stimulation. Graphs indicate the median ± IQR. Black horizontal lines in b indicate signaling threshold for each arcsinh transformed value. Black dotted boxes in b indicate clusters for which the arcsinh transformed median mass intensity surpassed the signaling threshold (±0.2-fold change) in either the C-GBM or NC-GBM cohort). A Student's T test with Bonferroni's correction for multiple comparisons was used to test for statistical significance. * = $p<0.05$, ** = $p<0.01$, *** = $p<0.001$, **** = $p <0.0001$.